



# Growth kinetics, metabolite yield, and expression analysis of biosynthetic pathway genes in friable callus cell lines of *Rhodiola imbricata* (Edgew)

Shiv Rattan<sup>1,2</sup> · Dinesh Kumar<sup>2,3</sup> · Ashish R. Warghat<sup>1,2</sup>

Received: 22 December 2020 / Accepted: 16 March 2021 / Published online: 25 March 2021  
© The Author(s), under exclusive licence to Springer Nature B.V. 2021

## Abstract

The plant cell culture provides an efficient technique for growth and production kinetics studies of bioactive compounds present in plants. Therefore, the present study investigated, for the first time, to identify the specific culture days required for higher metabolite yield in *Rhodiola imbricata*. A transcript-level gene expression study was conducted to understand the molecular cues associated with metabolite biosynthesis. The leaf callus cell line showed an optimum growth rate (FW: 20 g/100 mL, DW: 1.21 g/100 mL), growth index (19.00), salidroside (3.68 mg/g DW, rosavin (0.21 mg/g DW and rosarin (0.08 mg/g DW) on 24th day of the incubation period. However, salidroside, rosavin, and rosarin metabolite yield followed the growth-dependent manner in both callus cell lines, while tyrosol and *p*-coumaric acid showed growth independent accumulation pattern. Moreover, the antioxidant study displayed maximum phenolic content (8.07 mg/g DW) on day 18, flavonoid content (9.73 mg/g DW) on day 3, and DPPH activity ( $IC_{50}$ ; 0.79 mg/mL) on day 24 in leaf callus cell line. The RT-qPCR analysis showed upregulation of *PAL*, *4-HPAAS*, *4-HPAAR*, and *UDPGT* genes associated with metabolite accumulation. Expression analysis revealed a positive correlation with the metabolites yield. Furthermore, the optimized parameter could be exploited for a higher yield of specific metabolite and sequential scale-up studies.

## Key message

This is the first-ever study on the specific growth phase and accumulation pattern of metabolites in the friable callus cell lines of *Rhodiola imbricata*. Similarly, molecular signatures were also investigated to elucidate key genes associated with salidroside and rosavins biosynthesis. Furthermore, current optimized parameters lay the foundation for a cell suspension study, scale-up, and year-round metabolite production.

**Keywords** Antioxidant potential · Callus cell line · Growth kinetics · Salidroside yield · RT-qPCR · *Rhodiola imbricata*

Communicated by So-Young Park.

✉ Ashish R. Warghat  
ashishwarghat@ihbt.res.in; ashishwarghat@hotmail.com

Shiv Rattan  
shivrattan.negi@gmail.com

Dinesh Kumar  
dineshkumar@ihbt.res.in

<sup>1</sup> Biotechnology Division, CSIR-Institute of Himalayan Bioresource Technology, Palampur, Himachal Pradesh 176061, India

<sup>2</sup> Academy of Scientific and Innovative Research (AcSIR), Ghaziabad 201002, India

<sup>3</sup> Chemical Technology Division, CSIR-Institute of Himalayan Bioresource Technology, Palampur, Himachal Pradesh 176061, India

## Introduction

The majority of secondary metabolites predominantly derive from the plants and counterparts in the medicinal, agricultural, and industrial sectors. *Rhodiola imbricata* (Edgew) is a trans-Himalayan medicinal plant with immense pharmaceutical potential. The plant is used in a traditional therapeutic system and as a food crop (Choudhary et al. 2015; Tayade et al. 2017). *Rhodiola* is one of the richest salidroside sources and offers a commercially viable raw material for the herbal, health, and pharmaceutical industries. *R. imbricata* is sanctified with a plethora of pharmaceutical properties, viz., radioprotective, wound healing, freeze tolerance, anti-ageing, antioxidant, stress buster, immunomodulatory, and most

importantly, as an adaptogen (Chaurasia et al. 2003; Arora et al. 2005; Chawla et al. 2010; Tayade et al. 2013; Bhardwaj et al. 2018a; Tao et al. 2018; Kapoor et al. 2019; Rattan et al. 2020). Studies on *R. imbricata* showed the presence of dietary minerals, essential amino acids, ascorbic acid, vitamins, and antioxidant compounds, thus unleashing it as a nutraceutical rich source (Tayade et al. 2017). Phenylethanoids (Salidroside and Tyrosol) along with phenylpropanoids (rosavin and rosarin) were previously quantified in field-grown, in vitro plants and callus culture by Bhardwaj et al. (2018b), Bhardwaj et al. (2018c), Kapoor et al. (2018) and Rattan et al. (2020). These phyto complexes play a vital role in their remarkable biological potential and therefore draw significant scientific interest in *Rhodiola*. However, overexploitation and traditional usage of this herb persuaded threat to its wild habitat and receded this plant to red data book, hence became endemic and endangered (Kumar et al. 2011).

Due to the increment rise in demand for *Rhodiola* raw extract and salidroside (Tayade et al. 2017), a need for a reliable, affirmative, and efficient strategy for producing these metabolites has been eagerly sought. Dependence on field-grown plants for these secondary metabolites has conceded with ever-changing climatic conditions, poor seed germination, geographical barriers, plant growth cycle, and habitat loss (Chaurasia et al. 2007; Kumar et al. 2011). Therefore, to compensate for these impairments, an efficient protocol of in vitro seed germination, plant regeneration, and micropropagation techniques have been developed by Bhardwaj et al. (2018b), Bhardwaj et al. (2018c), and Rattan et al. (2020). Plant cell culture techniques were developed previously to produce metabolites in *R. imbricata* (Kapoor et al. 2018; Rattan et al. 2020). Further, cell culture offers an alternative strategy to produce the desired metabolite and reduce the burden on natural *Rhodiola* reserves. However, bioactive production through cell cultures in *R. imbricata* is still limited. Hence, there is a need to develop an optimized parameter for the sustainable production of desired metabolites.

Callus growth kinetics studies are significant for identifying the appropriate time for the passage and accumulation of bioactive substances. Thus, it facilitates the monitoring of callus culture, particularly biomass accumulation, cellular growth maintenance, and metabolites tracking (Costa et al. 2015). Reduction of nutrients, depletion of carbon sources, water availability, and the accumulation of toxic substances may reduce growth and starts browning of callus (Partap et al. 2020; Parsad et al. 2020; Wahyuni et al. 2020). Correspondingly, these parameters become pivotal in determining the overall growth period of callus cultures and maintaining logarithmic growth of cells (Nogueira et al. 2008). Similarly, dry callus growth kinetics are prudent for industrial applications, as dry biomass is more stable than fresh biomass (Costa et al. 2015). Likewise, investigating the

active involvement of genes related to metabolite biosynthesis opens various possibilities to validate and comprehend the overall flux of gene expression at different growth levels (Kumar et al. 2020; Rattan et al. 2020; Partap et al. 2020). Thus, the simultaneous evaluation of metabolite accumulation and gene expression can be assessed for proper harvesting and sustainable production. Increment in callus growth to culture days provides valuable insights about the accumulation behaviour of metabolites. Therefore, the present study focuses on the effective use of friable leaf and root callus cell line for callus growth rate, biomass, and metabolite yield with specific culture days by evaluating it through growth kinetics dynamics. Further, antioxidant profiling provides better evidence about the antioxidant potential of the *Rhodiola* callus extracts. Additionally, the investigation was carried out to elucidate pathway genes associated with salidroside, rosavin, and rosarin biosynthesis.

## Materials and methods

### Development and maintenance of friable callus cell line

The induction, proliferation, and establishment of friable green callus cell lines derived from in vitro leaf and root explants of *Rhodiola imbricata* were discussed in our previous report (Rattan et al. 2020). The friable callus cell lines were maintained on the MS medium augmented with previously standardized hormone concentrations of 0.5 mg/L TDZ and 1.0 mg/L NAA. Subsequently, callus cell lines were regularly subcultured at 25–30 day intervals and incubated under 25 °C temperature, 65% relative humidity, and 16 h light/8 h dark photoperiod with 70  $\mu\text{mol}/\text{m}^2/\text{s}$  light intensity.

### Callus cell growth and biomass yield

In the present investigation, actively growing friable green calli assessed for cell growth and biomass yield in *R. imbricata*. For growth kinetics study, 3 g callus as initial inoculum was used from the friable green callus. After that, callus was harvested every three-day interval up to 30 days of the incubation period in both callus cell lines. Also, fresh weight (FW) was measured for callus growth over the initial inoculum weight, and total callus growth biomass was recorded in terms of growth index (GI). All the harvested callus samples were dried in the oven at 35 °C and measured for callus dry weight (DW) determination. All the experiments were repeated thrice, and growth measurements were done with three replicates per harvesting day. GI was calculated using the formula described by Godoy-Hernandez and Vazquez-Flota (2006) as; Growth Index (GI) = final callus fresh

weight (FW) – initial callus fresh weight (FW)/initial callus fresh weight (FW). Callus biomass yield was expressed as gram per litre of medium, culture growth over the 30 days of the incubation period.

### Phytochemical extraction and UPLC-PDA analysis for determination of metabolite content and yield

The powdered callus samples (200 mg) were infused with 6 mL methanol (70%) and then kept in a water bath sonicator for 30 min. Afterward, extracts were centrifuged at 3500 rpm for 8 min at 4 °C and then filtered with a 0.22 µm PTFE syringe filter. Ultra-performance liquid chromatography (UPLC) equipped with a photodiode array (PDA) detector was used for metabolite quantification (Rattan et al. 2020). The quantification of major metabolites (salidroside, tyrosol, rosavin, and rosarin) with phenolic acids (gallic acid, *p*-coumaric acid, and cinnamic acid) was carried out in callus samples of *R. imbricata*. The gradient elution contains mobile phase A (0.1% formic acid in water), and mobile phase B (0.1% formic acid in acetonitrile) was used. The initial sample run was 3.0 min and 12 min for total run time, with detection wavelength set at 270 nm. Injection volume (1 µL) of the extract was used to estimate each marker compound, and metabolite yield was expressed as gram per culture days for one litre medium.

### Antioxidant assays

#### Total phenolic content (TPC)

Determination of TPC was done according to the protocol followed by Partap et al. (2019). Folin-Ciocalteu's (FC) reagent (1.5 mL) was added to 100 µL of methanolic extract of callus samples and incubated at room temperature for 5 min. After that, 1.2 mL of 2.5% Na<sub>2</sub>CO<sub>3</sub> solution was mixed into the reaction mixture and further incubated for 1 h. The absorbance was measured at 765 nm using a microplate reader against the blank. TPC was calculated as gallic acid equivalent (GAE) mg/g of callus dry extract. Concentrations (5–50 µg/µL) of gallic acid standard solutions was used for the plotting of calibration curve based on regression equation ( $y = 0.0579x - 0.1703$ ,  $R^2 = 0.998$ ).

#### Total flavonoid content (TFC)

Determination of TFC was done using the protocol followed by Partap et al. (2019). Each sample extract (100 µL) was mixed with 150 µL of NaNO<sub>2</sub> (0.5 M) and 150 µL of AlCl<sub>3</sub> (0.3 M). Afterward, 1.0 mL of 1 M NaOH solution was further mixed into the respective reaction mixture. The mixture was mixed thoroughly and incubated for 30 min. The absorbance was measured at 510 nm using a microplate reader

against blank. For TFC estimation, 20–100 µg/µL concentrations of quercetin were used for calibration curve preparation with regression equation ( $y = 0.0187x + 0.1864$ ,  $R^2 = 0.996$ ).

#### Free radical scavenging assay (DPPH)

DPPH activity of sample extract was evaluated as described previously by Kumar et al. (2020). A methanolic stock solution of 400 µM DPPH was prepared and kept at 10 °C for further use. Varying concentrations (200–240 µg/µL) of the sample extract were used, and made the final volume (1.0 mL) with the methanol in each reaction mixture. Afterward, 2.0 mL of DPPH solution was mixed with the respective extract. An equal volume of methanol (1.0 mL) and DPPH (2.0 mL) were used as a control. After that, the reaction mixture was incubated in the dark for 30 min. The absorbance was measured using a microplate reader at 517 nm. The IC<sub>50</sub> value of each sample extract and the standard was calculated to determine free radicle scavenging activity.

#### RNA extraction, cDNA preparation, and RT-qPCR analysis

Total RNA was isolated from callus samples on each harvesting day using the iRIS method (Ghawana et al. 2011). The integrity and quality of RNA were assessed by using NanoDrop™2000 (Thermo Scientific, USA). Verso cDNA synthesis kit was used for the preparation of the first strand cDNA as per the manufacturer's instructions. Previously designed primers of salidroside and rosavins biosynthetic pathway genes; Phenylalanine ammonia-lyase (*PAL*), Tyrosine decarboxylase (*TyDC*), 4-Hydroxyphenylacetaldehyde synthase (*4-HPAAS*), 4-Hydroxyphenylacetaldehyde reductase (*4-HPAAR*), Uridine 5'-diphospho-glucosyltransferase (*UDPGT*) were used for RT-qPCR analysis (Ma et al. 2008; Lan et al. 2013; Torrens-spence et al. 2018; Rattan et al. 2020) (Supplementary file; Table S1). Identical qPCR cycles were executed as 10 min at 94 °C (initial denaturation), 40 cycles of 94 °C for 15 s (denaturation), 52 °C to 56 °C (annealing temperature) for 30 s, extension at 72 °C for 30 s. Further, the 26S *rRNA* was used as an internal control for the normalization of data. Further, the 2<sup>(-ΔΔC<sub>t</sub>)</sup> method was used for the calculations (Schmittgen and Livak 2008).

#### Experimental data analysis

SPSS 25.0.0 software was used for the analysis of the experimental data. One-way ANOVA with Duncan and Dennett's test was done to evaluate significant differences among the studied parameter. Principal component analysis (PCA) was used for the comparison of significant differences among all studied characters. Multidimensional scaling (MDS)

analysis was used to ordinate all samples into clusters based on the studied parameters.

## Results

### Growth kinetics and metabolite accumulation

Time course breakdown of *R. imbricata* friable callus growth with respect to metabolite accumulation investigated for the first time. Fresh callus of leaf and root were harvested, weighed, and dried for dry mass estimation. The measured parameters (FW and DW) were described in callus biomass

per 100 mL medium. On day 27, maximum callus biomass FW (21.90 g, 18.72 g) and DW (1.21, 0.83 g) were observed in both callus lines (Tables 1, 2; Fig. 1). Correspondingly, up to day 24, the growth phase indicated a constant increase in leaf callus and ranged from 3.75 to 20.00 g FW. A similar pattern of growth was also seen in root callus, day 3 (3.59 g FW), and day 24 (18.04 g FW) (Tables 1, 2). However, from day 24 onwards stationary phase was observed and weighted 21.90 g FW on day 27 and 21.89 g FW on day 30 in the leaf callus (Table 1). In root callus, stationary phase was also observed on day 27 (18.72 g FW) and day 30 (18.40 g FW), respectively (Table 2). Similarly, dry weight (DW) in leaf callus was ranged from 0.24 to 1.21 g and in root callus

**Table 1** Growth biomass, growth index, and metabolite accumulation in leaf callus cell line of *R. imbricata* with respect to culture days

Culture days	Biomass production (g/100 mL)		GI	Metabolite content (mg/g DW)				
	FW	DW		Salidroside	Tyrosol	Rosavin	Rosarin	<i>p</i> -coumaric acid
3	3.75 ± 0.28 <sup>a</sup>	0.24 ± 0.01 <sup>a</sup>	2.75 ± 0.28 <sup>a</sup>	0.89 ± 0.01 <sup>a</sup>	0.82 ± 0.02 <sup>b,c</sup>	0.15 ± 0.00 <sup>b</sup>	0.04 ± 0.00 <sup>a</sup>	0.09 ± 0.00 <sup>a,b</sup>
6	6.04 ± 0.47 <sup>b</sup>	0.35 ± 0.02 <sup>b</sup>	5.04 ± 0.47 <sup>b</sup>	1.13 ± 0.00 <sup>b</sup>	0.86 ± 0.02 <sup>d,e</sup>	0.15 ± 0.00 <sup>b</sup>	0.04 ± 0.00 <sup>a</sup>	0.09 ± 0.00 <sup>a,b</sup>
9	7.93 ± 0.42 <sup>c</sup>	0.43 ± 0.01 <sup>bc</sup>	6.93 ± 0.42 <sup>c</sup>	1.97 ± 0.03 <sup>d</sup>	0.87 ± 0.02 <sup>c,d</sup>	0.18 ± 0.01 <sup>c</sup>	0.05 ± 0.00 <sup>a,b</sup>	0.09 ± 0.00 <sup>a,b</sup>
12	10.97 ± 0.41 <sup>d</sup>	0.50 ± 0.02 <sup>c</sup>	9.97 ± 0.41 <sup>d</sup>	2.43 ± 0.02 <sup>e</sup>	0.81 ± 0.00 <sup>b</sup>	0.19 ± 0.00 <sup>c</sup>	0.05 ± 0.00 <sup>a,b</sup>	0.10 ± 0.00 <sup>b</sup>
15	12.64 ± 0.24 <sup>e</sup>	0.70 ± 0.01 <sup>d</sup>	11.64 ± 0.24 <sup>e</sup>	2.78 ± 0.03 <sup>f</sup>	0.81 ± 0.01 <sup>b</sup>	0.19 ± 0.00 <sup>c</sup>	0.06 ± 0.00 <sup>b,c</sup>	0.08 ± 0.00 <sup>a</sup>
18	15.83 ± 0.10 <sup>f</sup>	0.86 ± 0.01 <sup>e</sup>	14.83 ± 0.10 <sup>f</sup>	3.11 ± 0.00 <sup>g</sup>	0.91 ± 0.00 <sup>d,e</sup>	0.19 ± 0.00 <sup>c</sup>	0.05 ± 0.00 <sup>a,b</sup>	0.11 ± 0.00 <sup>c</sup>
21	17.76 ± 0.13 <sup>g</sup>	0.92 ± 0.01 <sup>e</sup>	16.76 ± 0.13 <sup>g</sup>	3.14 ± 0.05 <sup>g</sup>	0.95 ± 0.01 <sup>e</sup>	0.19 ± 0.01 <sup>c</sup>	0.05 ± 0.00 <sup>a,b</sup>	0.11 ± 0.01 <sup>c</sup>
24	20.00 ± 0.10 <sup>h</sup>	1.21 ± 0.07 <sup>f</sup>	19.00 ± 0.10 <sup>h</sup>	3.68 ± 0.01 <sup>h</sup>	1.05 ± 0.03 <sup>f</sup>	0.21 ± 0.00 <sup>d</sup>	0.08 ± 0.00 <sup>d</sup>	0.14 ± 0.00 <sup>d</sup>
27	21.90 ± 0.14 <sup>i</sup>	1.21 ± 0.03 <sup>f</sup>	20.90 ± 0.14 <sup>i</sup>	2.03 ± 0.00 <sup>d</sup>	0.66 ± 0.01 <sup>a</sup>	0.17 ± 0.01 <sup>c</sup>	0.07 ± 0.00 <sup>c</sup>	0.09 ± 0.00 <sup>a,b</sup>
30	21.89 ± 0.46 <sup>i</sup>	1.20 ± 0.04 <sup>f</sup>	20.89 ± 0.46 <sup>i</sup>	1.75 ± 0.00 <sup>c</sup>	0.65 ± 0.01 <sup>a</sup>	0.11 ± 0.01 <sup>a</sup>	0.06 ± 0.01 <sup>b,c</sup>	0.08 ± 0.00 <sup>a</sup>

Experimental data represent the means of three replicates and standard error (SE). Different superscripts letters in a column specify statistically significant differences ( $p \leq 0.05$ , Duncan Multiple Range Test)

FW fresh weight, DW dry weight, GI growth index

**Table 2** Growth biomass, growth index, and metabolite accumulation in root callus cell line of *R. imbricata* with respect to culture days

Culture days	Biomass production (g/100 mL)		GI	Metabolite content (mg/g DW)				
	FW	DW		Salidroside	Tyrosol	Rosavin	Rosarin	<i>p</i> -coumaric acid
3	3.59 ± 0.10 <sup>a</sup>	0.21 ± 0.01 <sup>a</sup>	2.59 ± 0.10 <sup>a</sup>	1.18 ± 0.01 <sup>a</sup>	0.47 ± 0.02 <sup>b</sup>	0.07 ± 0.00 <sup>a,b</sup>	0.04 ± 0.00 <sup>a</sup>	0.09 ± 0.00 <sup>a,b,c</sup>
6	5.83 ± 0.07 <sup>b</sup>	0.33 ± 0.01 <sup>b</sup>	4.83 ± 0.07 <sup>b</sup>	1.28 ± 0.00 <sup>b</sup>	0.84 ± 0.03 <sup>c</sup>	0.08 ± 0.00 <sup>a,b</sup>	0.06 ± 0.00 <sup>b</sup>	0.09 ± 0.00 <sup>a,b</sup>
9	7.13 ± 0.06 <sup>c</sup>	0.45 ± 0.01 <sup>c</sup>	6.13 ± 0.06 <sup>c</sup>	1.47 ± 0.00 <sup>c</sup>	0.88 ± 0.01 <sup>c,d</sup>	0.08 ± 0.01 <sup>a,b,c</sup>	0.07 ± 0.00 <sup>b</sup>	0.09 ± 0.01 <sup>a,b,c</sup>
12	8.44 ± 0.13 <sup>d</sup>	0.51 ± 0.00 <sup>d</sup>	7.44 ± 0.13 <sup>d</sup>	2.02 ± 0.03 <sup>e</sup>	0.87 ± 0.01 <sup>c,m,d</sup>	0.09 ± 0.00 <sup>b,c,d</sup>	0.07 ± 0.01 <sup>b</sup>	0.11 ± 0.00 <sup>d,e</sup>
15	11.63 ± 0.13 <sup>e</sup>	0.64 ± 0.01 <sup>e</sup>	10.63 ± 0.13 <sup>e</sup>	2.69 ± 0.00 <sup>g</sup>	0.91 ± 0.02 <sup>d</sup>	0.09 ± 0.00 <sup>c,d</sup>	0.07 ± 0.01 <sup>b</sup>	0.10 ± 0.00 <sup>b,c,d</sup>
18	14.31 ± 0.18 <sup>f</sup>	0.72 ± 0.02 <sup>f</sup>	13.31 ± 0.18 <sup>f</sup>	2.95 ± 0.00 <sup>h</sup>	0.99 ± 0.01 <sup>e</sup>	0.12 ± 0.01 <sup>e</sup>	0.08 ± 0.00 <sup>b</sup>	0.10 ± 0.00 <sup>c,d</sup>
21	16.10 ± 0.11 <sup>g</sup>	0.78 ± 0.01 <sup>g</sup>	15.10 ± 0.11 <sup>g</sup>	2.97 ± 0.03 <sup>h</sup>	1.02 ± 0.02 <sup>e,f</sup>	0.13 ± 0.01 <sup>e</sup>	0.08 ± 0.00 <sup>b</sup>	0.11 ± 0.00 <sup>d,e</sup>
24	18.09 ± 0.07 <sup>h</sup>	0.82 ± 0.01 <sup>h</sup>	17.09 ± 0.07 <sup>h</sup>	3.39 ± 0.00 <sup>i</sup>	1.07 ± 0.02 <sup>f</sup>	0.15 ± 0.01 <sup>f</sup>	0.10 ± 0.01 <sup>c</sup>	0.12 ± 0.00 <sup>e</sup>
27	18.72 ± 0.23 <sup>i</sup>	0.83 ± 0.02 <sup>h</sup>	17.72 ± 0.23 <sup>i</sup>	2.38 ± 0.00 <sup>f</sup>	0.88 ± 0.03 <sup>c,d</sup>	0.10 ± 0.01 <sup>d</sup>	0.05 ± 0.00 <sup>a</sup>	0.09 ± 0.00 <sup>a,b</sup>
30	18.40 ± 0.28 <sup>h,i</sup>	0.81 ± 0.02 <sup>h</sup>	17.40 ± 0.28 <sup>h,i</sup>	1.66 ± 0.01 <sup>d</sup>	0.13 ± 0.00 <sup>a</sup>	0.07 ± 0.00 <sup>a</sup>	0.04 ± 0.00 <sup>a</sup>	0.08 ± 0.00 <sup>a</sup>

Experimental data represent the means of three replicates and standard error (SE). Different superscripts letters in a column specify statistically significant differences ( $p \leq 0.05$ , Duncan Multiple Range Test)

FW fresh weight, DW dry weight, GI growth index



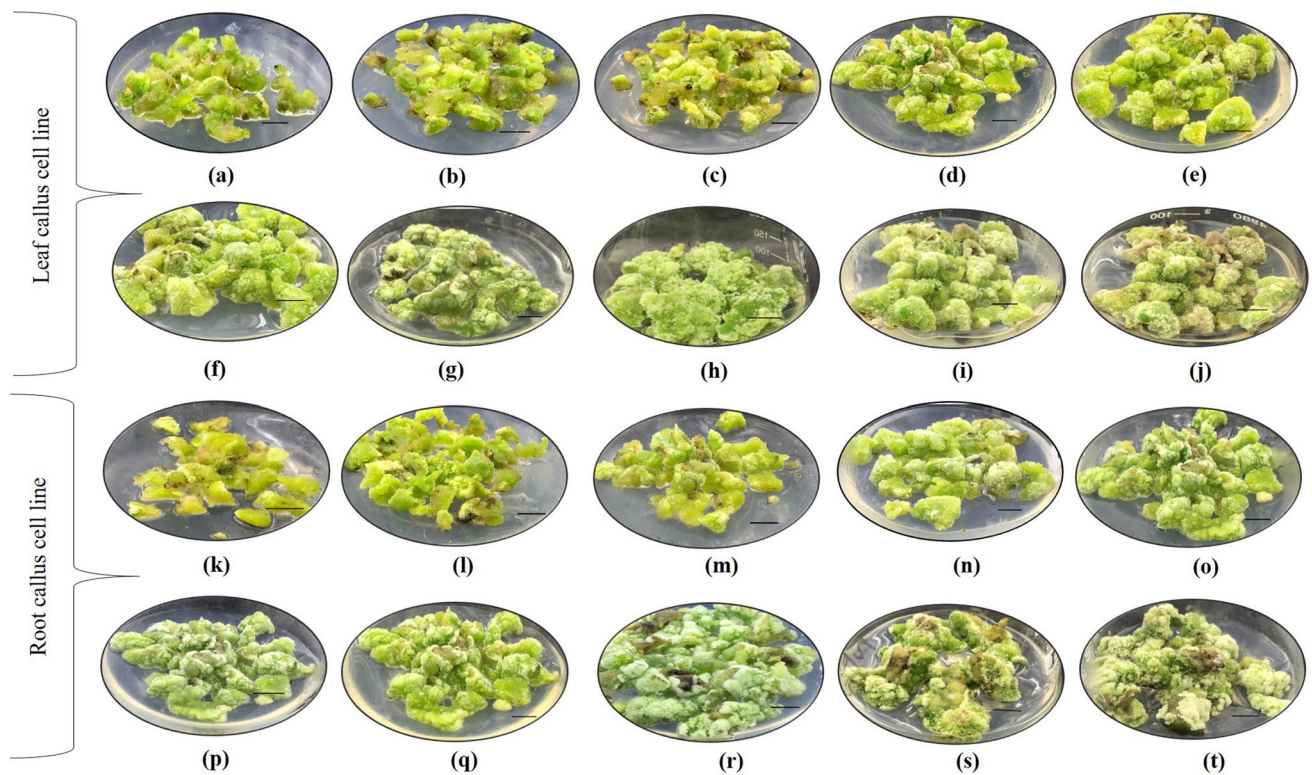


**Fig. 1** Successive stages of leaf and root callus cell line with respect to culture days in *R. imbricata*. Scale bar = 20 mm, **a–j** growth phases of leaf callus cell line; 3 days interval, **k–t** growth phases of root callus cell line; 3 days interval

0.21–0.82 g from day 3 to day 24. The stationary phase was observed on day 24 to day 30 in both calli (Tables 1, 2). Likewise, the growth index (GI) also followed a similar trend, as observed in callus growth biomass (Tables 1, 2). Both callus cell lines showed the highest growth index on day 27 (leaf; 20.90, root; 17.72) after a lag and exponential phase (Tables 1, 2).

Subsequently, culture day-wise metabolite accumulation in both callus cell lines was quantified. Maximum salidroside content was detected on day 24 (leaf; 3.68 mg/g DW, root; 3.39 mg/g DW), followed by day 21 (leaf; 3.14 mg/g DW, root; 2.97 mg/g DW) (Tables 1, 2).

Salidroside was detected at every successive harvesting day. Similarly, tyrosol was detected maximum on day 24; leaf callus (1.05 mg/g DW) and root callus (1.07 mg/g DW). However, a similar trend of accumulation was observed in both callus cell lines. The range varied from 0.65 to 1.05 mg/g DW in leaf callus, and root callus ranged from 0.47 to 1.07 mg/g DW (Tables 1, 2). Other key metabolites, rosavin, and rosarin followed a similar pattern in both callus cell lines. Rosavin was detected maximum on day 24 (0.21 mg/g DW) in leaf callus and (0.15 mg/g DW) in root callus. Moreover, rosarin was found maximum on day 21 in leaf callus (0.08 mg/g DW) and root callus (0.10 mg/g DW), respectively (Tables 1, 2). Overall, the accumulation

of these key metabolites was observed at every successive harvesting day in both callus cell lines (Supplementary file; Fig. S1 A to S1 U).

### Callus biomass production and metabolite yield

For the first time, friable leaf and root callus were studied to optimize culture days to obtain maximum metabolite yield. Subsequently, these optimized parameters are prerequisites for the scale-up of metabolite at shake flask and bioreactor level. Callus biomass production and net metabolite yield were expressed in g/L DW and g/culture days. Total callus biomass (g/L) and net salidroside yield (g/culture days) were predominantly calculated highest at day 24 (12.10 g/L; 44.53 g), followed by day 21 (9.20 g/L; 28.89 g) in leaf callus with respect to harvesting time (Fig. 2a). However, in root callus, maximum biomass accumulation yielded at day 27 (8.33 g/L), followed by day 24 (8.20 g/L), and net salidroside yield was 27.77 g on day 24, followed by day 21 (23.19 g), respectively (Fig. 2c). Furthermore, tyrosol achieved 12.75 g and 8.80 g in both callus cell lines on culture day 24 (Fig. 2a, c). However, rosavin and rosarin net yield were achieved the highest (2.48 g) and (1.04 g) in leaf callus on day 24. Similarly, in root callus, rosavin (1.24 g) and rosarin (0.79 g) were observed on the same day interval

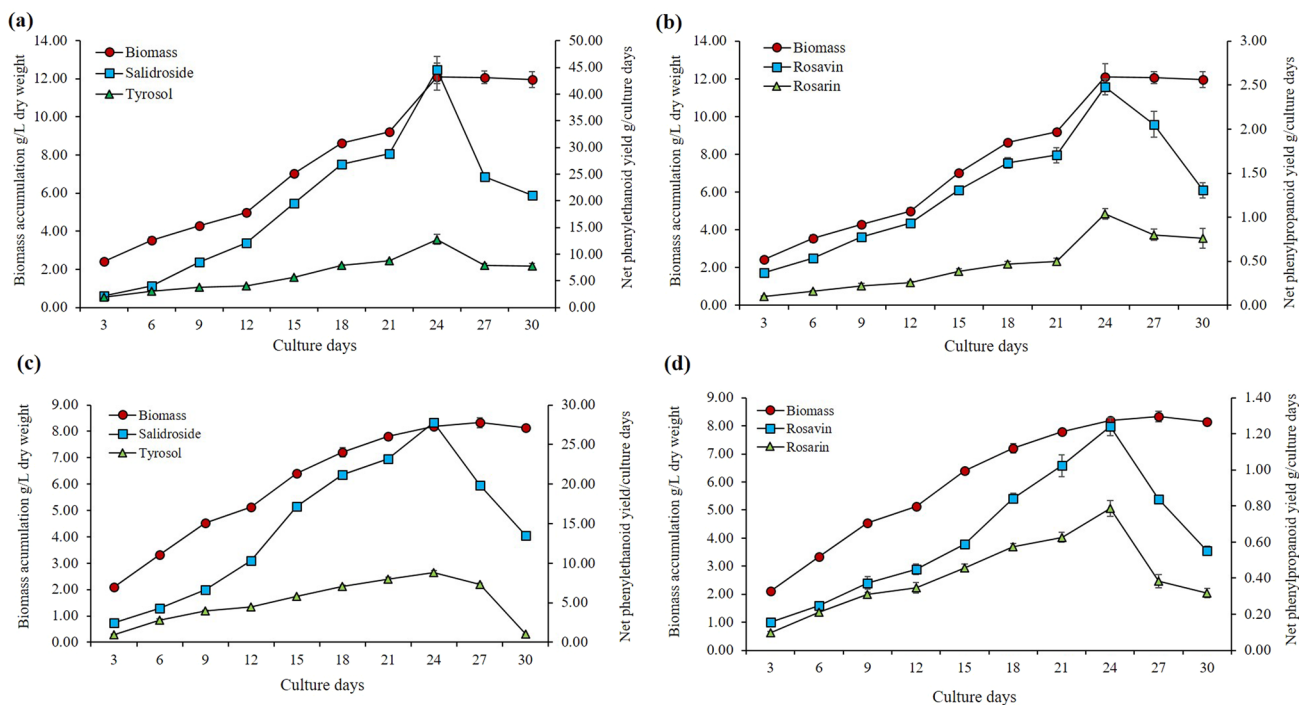


**Fig. 2** Time course of growth biomass and net metabolite yield in leaf and root callus cell line of *Rhodiola imbricata*. **a** and **b** biomass accumulation, phenylethanoid and phenylpropanoid yield in leaf cal-

lus cell line, **c** and **d** biomass accumulation, phenylethanoid and phenylpropanoid yield in root callus cell line

to total biomass (Fig. 2b, d). From the study, net salidroside and rosavins yield were obtained maximum on day 24, and after that, the reduced yield was observed.

### Total phenolic, flavonoid, and radical scavenging activity

TPC was accumulated maximum on culture day 18, i.e., 8.07 mg/g DW followed by day 24 (7.25 mg/g DW) in leaf callus (Table 3). However, in root callus, day 21 detected maximum TPC, i.e., 7.97 mg/g, followed by day 15 (7.41 mg/g DW), respectively (Table 4). Similarly, TFC was detected maximum in leaf callus on culture day 3, i.e., 9.73 mg/g, followed by day 30 (9.57 mg/g). Whereas root callus accumulated maximum TFC on culture day 24 (9.98 mg/g DW) followed by day 15 (8.97 mg/g DW), respectively (Table 4). Nevertheless, both callus cell lines showed an insignificant variation in TPC and TFC in the prospect of culture days. Furthermore, for the first time, a DPPH assay was done to evaluate the  $IC_{50}$ ,  $EC_{50}$ , ARP, and AEAC in both callus cell lines of *R. imbricata*. Lesser  $IC_{50}$  values indicate maximum scavenging activity, as a smaller amount of extract is needed to reduce the concentration of DPPH to 50%. Maximum scavenging activity i.e.,  $IC_{50}$  were detected in leaf callus on day 30 (0.79 mg/mL), and in root callus on day 9 (0.87 mg/mL) (Tables 3, 4). Similarly, DPPH

activity is also expressed as  $EC_{50}$  (mg/mL) and detected maximum in leaf callus (day 30; 2.39). While in root callus, day 9 showed higher  $EC_{50}$  values, i.e., 2.64. Moreover, ARP was observed maximum in leaf callus on day 24 (41.91) and in root callus on day 9 (37.93). Furthermore, AEAC was calculated (in mg AA/100 g) as 561.56 on day 24 in leaf callus, whereas in root callus, day 9 showed a maximum AEAC, i.e., 508.29 (Tables 3, 4). Overall, a disparate pattern was seen in both callus cell lines to culture days intervals.

### Gene expression pattern

On day-wise assessment, day 0 was considered as control, and subsequent days were considered treatments. The expression of genes in leaf callus was conjointly increased significantly on day 27, i.e., *PAL* (1.62-fold), *TYDC* (2.01-fold), *4-HPAAS* (5.04-fold), *4-HPAAR* (1.62-fold), and *UDPGT* (2.50-fold), respectively. Moreover, *4-HPAAR* showed significant transcript abundance on day 9 (3.63-fold), day 12 (3.42-fold), and day 30 (2.74-fold). In comparison, *UDPGT* showed maximum fold expression on day 12 (5.06-fold) and day 30 (3.33-fold) (Fig. 3a). Root callus showed a significant increase in transcript abundance of all five genes than control. Nevertheless, day 24 showed simultaneously increased RNA abundance for all genes as *PAL* showed transcript abundance of (3.30-fold), *TYDC*

**Table 3** Antioxidant activity of leaf callus cell line with respect to culture days in *R. imbricata*

Culture days	DPPH activity				TPC (mg gallic acid equivalent/g dry weight)	TFC (mg quercetin/g dry weight)
	IC <sub>50</sub> (mg/mL)	EC <sub>50</sub> (mg/mL)	ARP (%)	AEAC (mg AA/100 g)		
3	0.94 ± 0.01 <sup>b,c</sup>	2.86 ± 0.02 <sup>c</sup>	34.92 ± 0.21 <sup>b</sup>	468.02 ± 2.83 <sup>b</sup>	6.43 ± 0.06 <sup>c</sup>	9.73 ± 0.14 <sup>e</sup>
6	0.97 ± 0.02 <sup>b,c</sup>	2.95 ± 0.05 <sup>c</sup>	33.91 ± 0.51 <sup>b</sup>	454.42 ± 6.86 <sup>b</sup>	6.35 ± 0.11 <sup>c</sup>	9.51 ± 0.06 <sup>d,e</sup>
9	0.93 ± 0.02 <sup>b</sup>	2.83 ± 0.06 <sup>c</sup>	35.39 ± 0.73 <sup>b</sup>	474.29 ± 9.81 <sup>b</sup>	6.52 ± 0.05 <sup>c</sup>	6.16 ± 0.04 <sup>a</sup>
12	0.94 ± 0.03 <sup>b,c</sup>	2.83 ± 0.08 <sup>c</sup>	35.37 ± 0.94 <sup>b</sup>	473.96 ± 12.62 <sup>b</sup>	5.55 ± 0.04 <sup>b</sup>	9.36 ± 0.17 <sup>d,e</sup>
15	1.06 ± 0.00 <sup>d</sup>	3.22 ± 0.00 <sup>d</sup>	31.10 ± 0.04 <sup>a</sup>	416.75 ± 0.49 <sup>a</sup>	7.12 ± 0.12 <sup>e</sup>	8.26 ± 0.35 <sup>b,c</sup>
18	0.83 ± 0.00 <sup>a</sup>	2.52 ± 0.00 <sup>b</sup>	39.62 ± 0.05 <sup>c</sup>	530.98 ± 0.62 <sup>c</sup>	8.07 ± 0.05 <sup>f</sup>	8.25 ± 0.24 <sup>b,c</sup>
21	0.83 ± 0.00 <sup>a</sup>	2.51 ± 0.01 <sup>b</sup>	39.91 ± 0.13 <sup>c</sup>	534.77 ± 1.76 <sup>c</sup>	5.06 ± 0.02 <sup>a</sup>	7.95 ± 0.12 <sup>b</sup>
24	0.79 ± 0.01 <sup>a</sup>	2.39 ± 0.03 <sup>a</sup>	41.91 ± 0.58 <sup>d</sup>	561.56 ± 7.78 <sup>d</sup>	7.25 ± 0.05 <sup>e</sup>	7.87 ± 0.12 <sup>b</sup>
27	0.98 ± 0.02 <sup>d</sup>	2.96 ± 0.05 <sup>c</sup>	33.86 ± 0.58 <sup>b</sup>	453.80 ± 7.74 <sup>b</sup>	6.76 ± 0.11 <sup>d</sup>	8.83 ± 0.06 <sup>c,d</sup>
30	0.79 ± 0.00 <sup>a</sup>	2.39 ± 0.01 <sup>a</sup>	41.82 ± 0.23 <sup>d</sup>	560.43 ± 3.08 <sup>d</sup>	6.75 ± 0.04 <sup>d</sup>	9.57 ± 0.61 <sup>d,e</sup>

Experimental data represent the means of three replicates and standard error (SE). Different superscripts letters in a column specify statistically significant differences ( $p \leq 0.05$ , Duncan Multiple Range Test)

DPPH-2,2-diphenyl-1-picrylhydrazyl

IC<sub>50</sub>-half maximal inhibitory concentration, EC<sub>50</sub>-half-maximal effective concentration

ARP-antiradical power =  $(1/EC_{50}) \times 100$

AEAC-ascorbic acid equivalent antioxidant capacity =  $(IC_{50(AA)}/IC_{50(sample)}) \times 10^5$

AA ascorbic acid

**Table 4** Antioxidant activity of root callus cell line with respect to culture days in *R. imbricata*

Culture days	DPPH activity				TPC (mg gallic acid equivalent/g dry weight)	TFC (mg quercetin/g dry weight)
	IC <sub>50</sub> (mg/mL)	EC <sub>50</sub> (mg/mL)	ARP (%)	AEAC (mg AA/100 g)		
3	0.91 ± 0.01 <sup>a,b</sup>	2.75 ± 0.03 <sup>a,b</sup>	36.38 ± 0.34 <sup>b</sup>	487.48 ± 4.52 <sup>b</sup>	6.55 ± 0.01 <sup>d</sup>	7.59 ± 0.17 <sup>b</sup>
6	0.96 ± 0.01 <sup>c</sup>	2.91 ± 0.03 <sup>c</sup>	34.40 ± 0.39 <sup>a</sup>	460.97 ± 5.15 <sup>a</sup>	5.67 ± 0.08 <sup>b</sup>	7.87 ± 0.22 <sup>b</sup>
9	0.87 ± 0.00 <sup>a</sup>	2.64 ± 0.01 <sup>a</sup>	37.93 ± 0.07 <sup>c</sup>	508.29 ± 0.97 <sup>c</sup>	6.63 ± 0.10 <sup>d,e</sup>	7.83 ± 0.09 <sup>b</sup>
12	0.96 ± 0.02 <sup>c</sup>	2.91 ± 0.05 <sup>c</sup>	34.39 ± 0.54 <sup>a</sup>	460.80 ± 7.18 <sup>a</sup>	6.82 ± 0.14 <sup>e</sup>	8.00 ± 0.18 <sup>b</sup>
15	0.94 ± 0.02 <sup>bc</sup>	2.85 ± 0.07 <sup>bc</sup>	35.08 ± 0.87 <sup>a</sup>	470.19 ± 11.61 <sup>a,b</sup>	7.41 ± 0.04 <sup>f</sup>	8.97 ± 0.32 <sup>c</sup>
18	0.94 ± 0.01 <sup>bc</sup>	2.86 ± 0.03 <sup>bc</sup>	34.96 ± 0.31 <sup>a</sup>	468.47 ± 4.16 <sup>a</sup>	6.31 ± 0.06 <sup>c</sup>	8.90 ± 0.12 <sup>c</sup>
21	0.98 ± 0.02 <sup>c</sup>	2.97 ± 0.06 <sup>c</sup>	33.66 ± 0.64 <sup>a</sup>	451.12 ± 8.56 <sup>a</sup>	7.97 ± 0.08 <sup>g</sup>	8.14 ± 0.23 <sup>b</sup>
24	0.98 ± 0.01 <sup>c</sup>	2.98 ± 0.03 <sup>c</sup>	33.57 ± 0.36 <sup>a</sup>	449.83 ± 4.80 <sup>a</sup>	6.19 ± 0.03 <sup>c</sup>	9.98 ± 0.21 <sup>d</sup>
27	0.97 ± 0.01 <sup>c</sup>	2.93 ± 0.03 <sup>c</sup>	34.19 ± 0.31 <sup>a</sup>	458.22 ± 4.10 <sup>a</sup>	4.08 ± 0.07 <sup>a</sup>	6.82 ± 0.12 <sup>a</sup>
30	0.96 ± 0.01 <sup>c</sup>	2.92 ± 0.02 <sup>c</sup>	34.23 ± 0.21 <sup>a</sup>	458.77 ± 2.87 <sup>a</sup>	4.07 ± 0.08 <sup>a</sup>	6.27 ± 0.12 <sup>a</sup>

Experimental data represent the means of three replicates and standard error (SE). Different superscripts letters in a column specify statistically significant differences ( $p \leq 0.05$ , Duncan Multiple Range Test)

DPPH-2,2-diphenyl-1-picrylhydrazyl

IC<sub>50</sub>-half maximal inhibitory concentration, EC<sub>50</sub>-half maximal effective concentration

ARP-antiradical power =  $(1/EC_{50}) \times 100$

AEAC-ascorbic acid equivalent antioxidant capacity =  $(IC_{50(AA)}/IC_{50(sample)}) \times 10^5$

AA ascorbic acid

(4.73-fold), 4-HPAAS (5.52-fold), 4-HPAAR (14.78-fold), and UDPGT (1.82-fold) respectively (Fig. 3b). Though, maximum expression of PAL (5.36-fold) was observed on day 12, followed by day 18 (4.33-fold). Similarly, TYDC showed maximum RNA expression on day 6 (6.10-fold) and

day 15 (5.57-fold). While, 4-HPAAS has increased transcript abundance on day 12 (8.86-fold), followed by day 27 (6.41-fold) and day 21 (5.62-fold), respectively. Likewise, UDPGT showed the highest expression on day 27 (4.09-fold), followed by day 6 (4.02-fold), day 15 (2.43-fold), and day 9

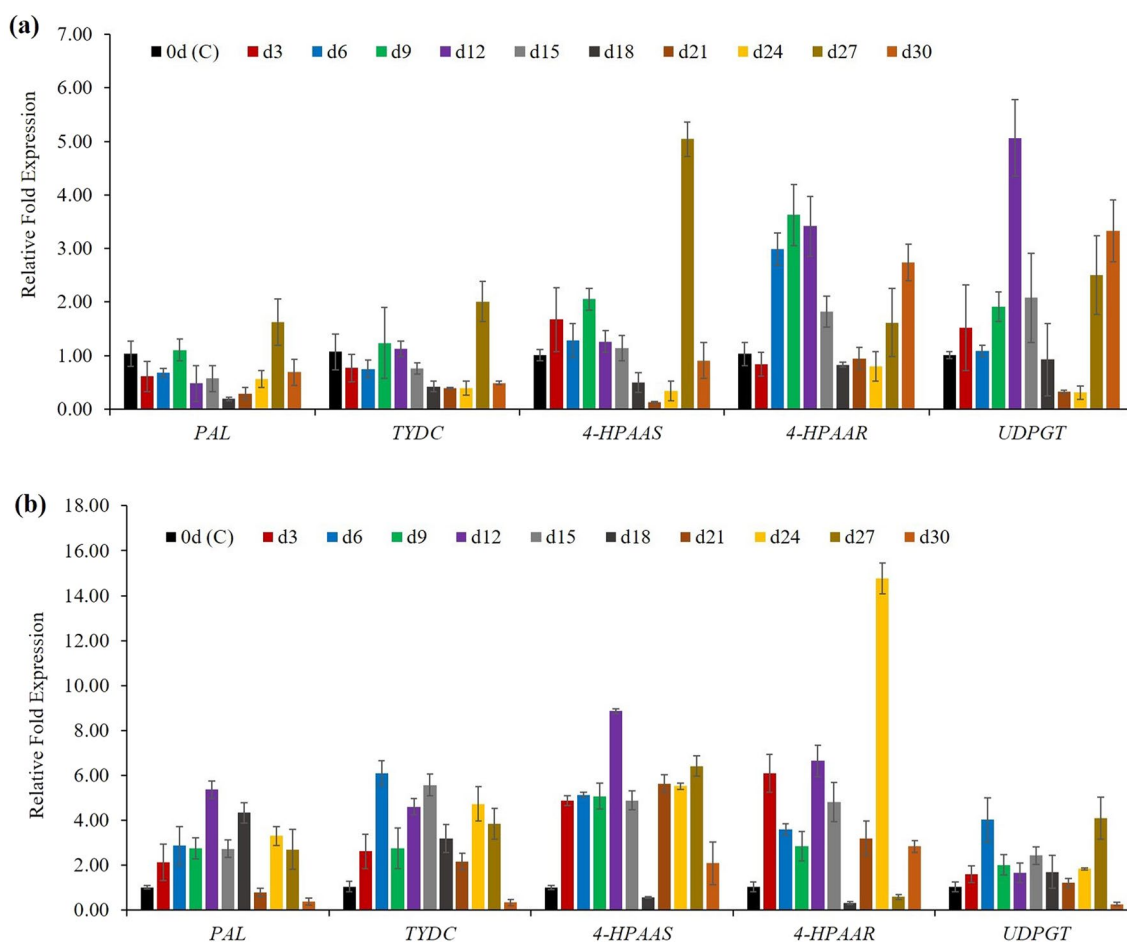


**Fig. 3** Expression profiling of phenylethanoid and phenylpropanoid pathway genes with respect to culture days in leaf and root callus cell line of *R. imbricata*. **a** leaf callus cell line, **b** root callus cell line. *PAL*; phenylalanine ammonia-lyase, *TYDC*; tyrosine decarboxy-

lase, *4-HPAAS*; 4-hydroxyphenylacetaldehyde synthase, *4-HPAAR*; 4-hydroxyphenylacetaldehyde reductase, *UDPGT*; UDP-glucosyltransferase. (Color figure online)

(2.00-fold) (Fig. 3b). In leaf callus, *4-HPAAR* and *UDPGT* showed increased expression on initial culture days than intermediate days and further showed higher expression at later days (Fig. 3a). The overall gene expression remained higher in the root callus and followed a relatively more or less pattern throughout the culture days (Fig. 3b).

### Correlation analysis

In leaf callus, component analysis extracted two PC axis with variation PC1 (31.54%) and PC2 (25.14%). Furthermore, the PC1 axis contained highly correlated characters such as FW, DW, and GI, while the PC2 axis contained TYR and *HPAAS* (Fig. 4a). In root callus, component analysis extracted PC1 (33.51%) and PC2 (25.72%) variation. Moreover, the PC1 axis accumulated FW, DW, GI, and DPPH activity (IC50, EC50, ARP, AEAC) as highly correlated characters. Likewise, the PC2 axis contained highly

correlated characters such as TFC, TYR, and ROR (Fig. 4b). The analysis found that test parameters in both callus cell lines unveiled two different PC axis presenting random illustrations. Additionally, multidimensional scaling (MDS) was used for cluster-wise allocation of test parameters based on the Euclidean distance model. In leaf callus, samples formed four clusters (Stress = 0.146; RSQ; 0.891). Where cluster I contain GA, IC50, and EC50. While cluster II denotes; ROV, TPC, TYR, SAL, PCOU, and ROR. Likewise, Cluster III depicts DW, GI, FW, AEAC, and ARP into one group. Though, cluster IV contains *HPAAS*, *TYDC*, *HPAAR*, *PAL*, *UDPGT*, and TFC, respectively (Fig. 4c). Similarly, four clusters were formed in root callus (Stress = 0.144; RSQ; 0.911). Where cluster I denote FW, DW, GI, IC50, and EC50. While GA, *UDPGT*, *HPAAS*, *TYDC*, and *PAL* resided in cluster II. Similarly, cluster III represents; TYR, TFC, *HPAAR*, TPC, PCOU, AEAC, and ARP. Further, SAL, ROV, and ROV were grouped into Cluster IV (Fig. 4d). The above



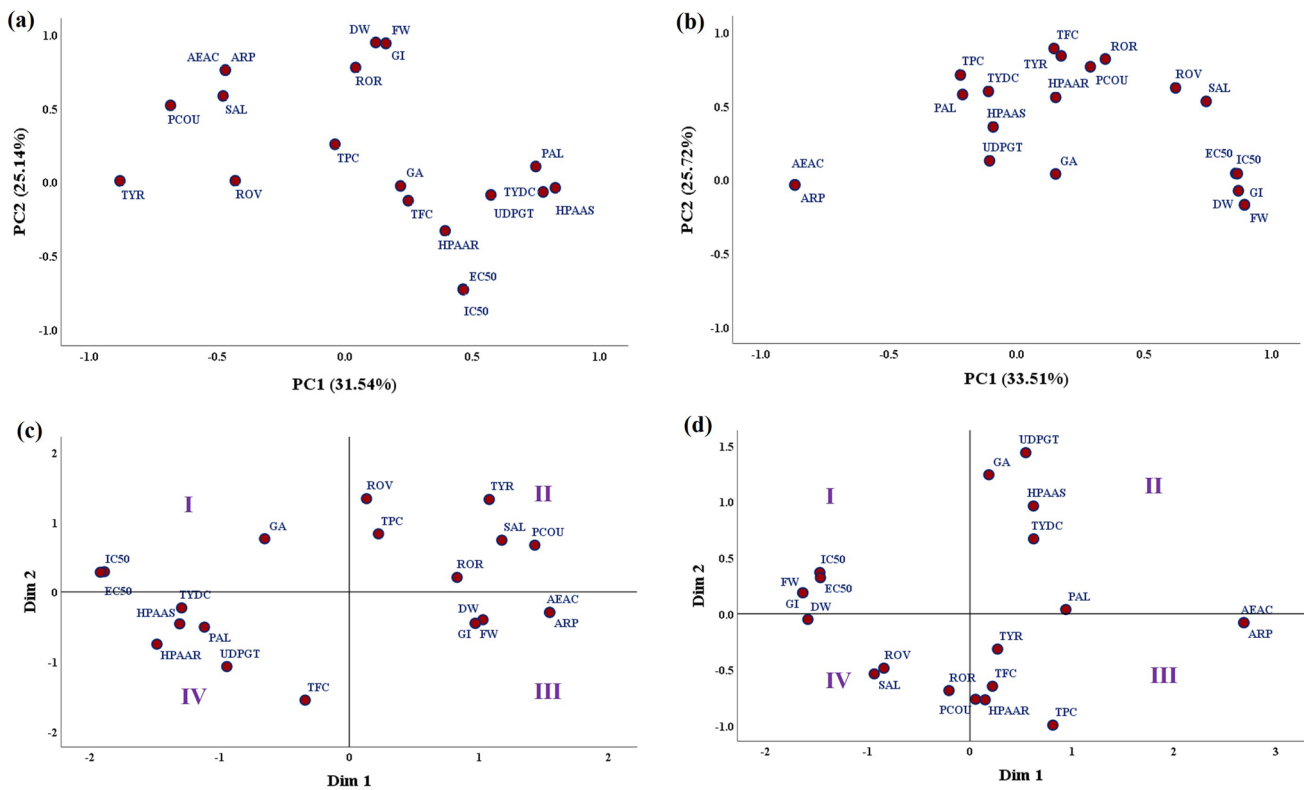


**Fig. 4** Correlation between growth biomass, growth index, metabolite content, antioxidant activity, and gene expression pattern in leaf and root callus cell line of *R. imbricata* with respect to culture days. **a** and **b** PCA analysis of leaf and root callus cell line, **c** and **d** MDS analysis of leaf and root callus cell line. FW-fresh weight; DW-dry weight; GI-growth index; GA-gallic acid; SAL-salidroside, TYR-tyrosol;

ROV-rosavin; ROR-rosarin; PCOU- *p*-coumaric acid; TPC- total phenolic content; TFC-total flavonoid content; DPPH activity (IC50, EC50, ARP, AEAC); PAL; phenylalanine ammonia-lyase, TYDC; tyrosine decarboxylase, 4-HPAAS; 4-hydroxyphenylacetaldehyde synthase, 4-HPAAR; 4-hydroxyphenylacetaldehyde reductase, UDPGT; UDP-glucosyltransferase

observation achieved dissimilarities between data variables and illustrated distinct clusters in both callus cell lines.

## Discussion

Callus growth rate and culture duration often play a vital role in the accumulation behaviour of metabolites. Thus, understanding the biosynthesis mechanism of natural products is essential for improving secondary metabolites yield (Hussein et al. 2016). Therefore, determining the specific growth phase with higher metabolite yield is the utmost significant criteria. This production strategy is broadly explored using callus, suspension, and in vitro cultures of medicinal plants (Alvarez 2014; Kapoor et al. 2019; Partap et al. 2020; Prasad et al. 2020). But studies related to salidroside production assessing growth dynamics of callus cell lines were still limited in *R. imbricata*. The present findings showed that the metabolite accumulation pattern was closely associated with actively growing callus cell lines. Production of salidroside reached the maximum at day 24 with vigorous callus

growth. Afterward, restricted callus growth was observed, leading to slightly oxidized patches. The overall callus morphology and colour remained the same until the stationary phase. Calli were further oxidized at the end of the stationary phase, leading to callus browning in patches. Oxidized brown patches have resulted from phenolic oxidation, which induces brown pigment formation (Coimbra et al. 2019). In general, cell growth curves are of the sigmoid type. In the present study, both callus cell lines showed a relatively fast growth in which the log phase was observed until day 24 of incubation. Nevertheless, biomass accumulation in the leaf callus cell line was higher than the root callus cell line. Several factors such as active cell division, more parenchymal cells, endogenous amounts of growth regulators, and efficient use of nutrients triggered the leaf callus cell line to proliferate faster than the root callus cell line (Rattan et al. 2020). To date, there is no previous literature available about growth kinetics study in root callus cell line of *R. imbricata*. However, growth and biomass studies in callus and suspension cultures of *R. imbricata* were previously reported by Kapoor et al. (2018, 2019).

In vitro production of desired metabolites has always been an interesting arena for researchers. It exhibits the potential to fulfill the ever-expanding commercial demands of plant phytochemicals on a sustainable basis (Efferth 2019). Although callus culture, suspension culture, adventitious root culture provides an efficient technique for metabolite production in *Rhodiola* species (Wu et al. 2003; Shi et al. 2013; Bhardwaj et al. 2018b, c; Kapoor et al. 2019; Mirmazloum et al. 2019; Rattan et al. 2020; Stepanova et al. 2021). The present study investigated callus cell lines for growth-related secondary metabolite production. These cell lines produced phenylethanoids and phenylpropanoids in an explant type and growth-dependent manner. The successive increment in metabolite production was observed in both callus cell lines with increasing callus growth. The outcomes revealed that the concentration of metabolites (mg/g) followed a close response pattern in both callus cell lines. However, the leaf callus cell line showed higher metabolites yield based on biomass accumulation (g/L) perspective. Further, the leaf callus cell line can be exploited for a sequential scale of metabolites at the suspension level. The present findings were in accordance with the previously published report of Kapoor et al. (2018) and Rattan et al. (2020). Growth-dependent metabolite production may have attributed to the low availability of sucrose, plant growth regulators, nitrogen source, and microelements at the later stage of the incubation period (Costa et al. 2015; Kapoor et al. 2019; Wahyuni et al. 2020). Benyammi et al. (2016) and Hundare et al. (2018) reported maximum metabolites accumulation at the post-exponential phase. The present investigation explained the higher metabolite yield in callus cell lines concerning specific time and growth rate. These findings may lay the firm foundation for active ingredient harvesting, production strategies, and further use of callus cell lines in suspension culture with nutrient and chemical feeding to improve the overall yield of desired metabolites.

The medicinal potential of the plants ascribed in the occurrence of phytochemicals with varying biological potential; therefore, it becomes necessary to evaluate the total phenolic and flavonoid content. In the present study, callus cell lines were assessed for the first time to identify antioxidant potential concerning the growth phase. The content of phenols, flavonoids, and radical scavenging activity showed an independent link with callus growth. Consequently, antioxidant potential varied in all subsequent culture days and ranged in close proximity to the initial culture days. Plant phenolics are carbon-based secondary compounds. Several biochemical and molecular studies strongly support the idea that plant phenol levels are positively correlated with the content of available photosynthesis and negatively correlated with plant growth and nutrient status (Nybakken et al. 2011). Similarly, Naik et al. (2010) reported that decreased phenolic compounds are associated with sucrose intake during

callus growth. Hence, periodic subcultures are necessary for the renewal of carbon sources for the construction of new molecules. Previously, Kapoor et al. (2018) assessed total phenolic (11.84 mg/g DW), total flavonoid (5.53 mg/g DW) content, and DPPH activity (53.50%) in leaf callus grown under blue light condition. However, in suspension culture treated with jasmonic acid (100 mM), enhanced production of total phenolic (14.69 mg/g DW), total flavonoid (4.95 mg/g DW) content, and DPPH scavenging activity (56.32%) in *R. imbricata* (Kapoor et al. 2019).

The active role of key genes in salidroside and rosavins production is previously studied in *Rhodiola* species (Ma et al. 2008; Zhang et al. 2011; Lan et al. 2013; Mirmazloum et al. 2015; Torrens-spence et al. 2018; Rattan et al. 2020). The present study emphasized evaluating the transcript-level expression of pathway genes in callus cell lines. Therefore, metabolite content was validated and correlated by RT-qPCR expression profiling of pathway genes. Obtained results revealed that *PAL*, *4-HPAAS*, *4-HPAAR*, and *UDPGT* genes are actively involved in the biosynthesis of metabolites and showed increased upregulation. The role of tyrosine decarboxylase (*TYDC*) and phenylalanine ammonia-lyase (*PAL*) in salidroside and rosavins biosynthesis was reported by Zhang et al. (2011) and Mirmazloum et al. (2015). Cui et al. (2017) studied the role of endophyte *Trimmatostroma* species in *R. crenulata*. They concluded the association of gene expression with salidroside production. Moreover, Torrens-spence et al. (2018) stated the active role of genes *4-HPAAS* and *4-HPAAR* in phenylpropanoid pathway in *R. rosea*. Furthermore, Rattan et al. (2020) recently reported the active involvement of all biosynthetic pathway genes in metabolite production. The current study suggests the correlation between metabolite production and increased expression of biosynthetic pathway genes in both callus cell lines.

Overall, callus biomass production and metabolite yield was achieved significantly higher on day 24 in both callus cell lines. Subsequently, expression analysis also revealed higher expression of biosynthetic pathway genes. This study can be further explored to enhance metabolite yield in *R. imbricata* through metabolic pathway engineering or genome editing tools.

## Conclusion

The present study is the first successful attempt for the callus biomass production with higher metabolite yield in friable callus cell lines of *R. imbricata*. Salidroside content achieved maximum at the exponential phase of the callus in the 30-day incubation period. Moreover, culture day 24 can be utilized for metabolite yield, further subculture, and suspension culture experiments. The metabolite produced higher in the leaf callus cell line, and further, it can be used

for pilot and commercial-scale metabolite production. This study also emphasizes the reduction in time duration for metabolite yield, which usually takes 3 to 5 years in the wild and is a vital consideration for future up-scaling efforts. This investigation may lay theoretical and practical foundations for further research on precursor and elicitor feeding, bioreactor scale-up studies, pathway modulation efforts, and commercial application in the cell culture of *R. imbricata*.

**Supplementary Information** The online version contains supplementary material available at <https://doi.org/10.1007/s11240-021-02057-8>.

**Acknowledgements** The authors acknowledge the Council of Scientific and Industrial Research (CSIR), Government of India, under the project “Biotechnological interventions for sustainable bio-economy generation through characterization, conservation, prospection and utilization of Himalayan bioresources (MLP-0201)” for providing financial support. SR acknowledges UGC, New Delhi for providing research fellowship and Academy of Scientific and Innovative Research (AcSIR), Ghaziabad, India for Ph. D. enrolment. The authors are thankful to Director, CSIR-IHBT, Dr. Sanjay Kumar, for providing the necessary facilities. CSIR-IHBT publication number for this manuscript is 4768.

**Author contributions** Conceptualization: SR and ARW; Methodology: SR and ARW; Data analysis and investigation: SR, DK, and ARW; Writing-original draft preparation, review and edition: SR and ARW.

## Declarations

**Conflict of interest** The authors declare that there is no conflict of interest.

**Ethical approval** Research article followed the ethical standard of the institute.

## References

- Alvarez MA (2014) Solasodine production in *Solanum eleagnifolium* in vitro cultures. Plant biotechnology for health. Springer, Cham
- Arora R, Chawla R, Sagar R, Prasad J, Singh S, Kumar R, Sharma A, Singh S, Sharma RK (2005) Evaluation of radioprotective activities of *Rhodiola imbricata* Edgew—a high altitude plant. Mol Cell Biochem 273:209–223
- Benyammi R, Paris C, Khelifi-Slaoui M, Zaoui D, Belabbassi O, Bakiri N, Meriem Aci M, Harfi B, Malik S, Makhzoum A, Desobry S, Khelifi L (2016) Screening and kinetic studies of catharanthine and ajmalicine accumulation and their correlation with growth biomass in *Catharanthus roseus* hairy roots. Pharm Biol 54:2033–2043
- Bhardwaj AK, Naryal A, Bhardwaj P, Warghat AR, Arora B, Saxena S, Pati PK, Chaurasia OP (2018a) High efficiency in vitro plant regeneration and secondary metabolite quantification from leaf explants of *Rhodiola imbricata*. Pharmacogn J 10:470–475
- Bhardwaj AK, Singh B, Kaur K, Roshan P, Sharma A, Dolker D, Naryal A, Saxena S, Pati PK, Chaurasia OP (2018b) In vitro propagation, clonal fidelity and phytochemical analysis of *Rhodiola imbricata* Edgew: a rare trans-Himalayan medicinal plant. Plant Cell Tiss Organ Cult 135:499–513
- Bhardwaj P, Bhardwaj G, Raghuvanshi R, Thakur MS, Kumar R, Chaurasia OP (2018c) Rhodiola: an overview of phytochemistry and pharmacological applications. New age herbals, 1st edn. Springer, Singapore, pp 71–113
- Chaudhary A, Kumar R, Srivastava RB, Surapaneni SK, Tikoo K, Singh IP (2015) Isolation and characterization of phenolic compounds from *Rhodiola imbricata*, a Trans-Himalayan food crop having antioxidant and anticancer potential. J Funct Foods 16:183–193
- Chaurasia OP, Ballabh B, Singh B (2003) Himalayan rose root, *Rhodiola* spp., potential health drink and drug plant. Nat Prod Rad 2:71–92
- Chaurasia OP, Ahmed Z, Ballabh B (2007) Ethnobotany and plants of Trans-Himalaya. Satish Serial Publishing House, New Delhi, pp 1–544
- Chawla R, Jaiswal S, Kumar R, Arora R, Sharma RK (2010) Himalayan Bioresource *Rhodiola imbricata* as a promising radioprotector for nuclear and radiological emergencies. J Pharm Bioallied Sci 2:213–219
- Coimbra MC, Chagas RCR, Vilela MSP, Castro AHF (2019) Growth, morphology and bioactive phenolic compounds production in *Pyrostegia venusta* calli. Biocatal Agric Biotechnol 18:101036
- Costa JDL, Silva ALLD, Bier MCJ, Brondani GE, Gollo AL, Letti LAJ, Erasmo EAL, Soccol CR (2015) Callus growth kinetics of physic nut (*Jatropha curcas* L.) and content of fatty acids from crude oil obtained in vitro. Appl Biochem Biotechnol 176(3):892–902
- Cui JL, Wang Y, Jiao J, Gong Y, Wang J, Wang M (2017) Fungal endophyte-induced salidroside and tyrosol biosynthesis combined with signal cross-talk and the mechanism of enzyme gene expression in *Rhodiola crenulata*. Sci Rep 7:12540
- Ghawana S, Paul A, Kumar H, Kumar A, Singh H, Bhardwaj PK, Rani A, Singh RS, Raizada J, Singh K, Kumar S (2011) An RNA isolation system for plant tissues rich in secondary metabolites. BMC Res Notes 4:1–5
- Godoy-Hernandez G, Vazquez-Flota FA (2006) Growth measurements: estimation of cell division and cell expansion. plant cell culture protocols, 2nd edn. Humana Press Inc, Totowa (NJ), pp 51–58
- Hundare A, Dhayதாக B, Kudale S, Joshi N (2018) Growth kinetics and diosgenin estimation from callus cultures of *Costus speciosus* (Koen. ex. Retz.). Nat Prod Res 32:1809–1816
- Hussein S, Halmi MIE, Ling APK (2016) Modelling the growth kinetics of callus cultures from the seedling of *Jatropha curcas* L. according to the modified gompertz model. J Microbiol Biotechnol 4:20–23
- Kapoor S, Raghuvanshi R, Bhardwaj P, Sood H, Saxena S, Chaurasia OP (2018) Influence of light quality on growth, secondary metabolites production and antioxidant activity in callus culture of *Rhodiola imbricata* Edgew. J Photochem Photobiol B 183:258–265
- Kapoor S, Sharma A, Bhardwaj P, Sood H, Saxena S, Chaurasia OP (2019) Enhanced production of phenolic compounds in compact callus aggregate suspension cultures of *Rhodiola imbricata* edgew. Appl Biochem Biotechnol 187:817–837
- Kumar GP, Kumar R, Chaurasia OP (2011) Conservation status of medicinal plants in Ladakh: cold arid zone of Trans-Himalayas. Res J Med Plants 5:685–694
- Kumar P, Partap M, Ashrita RD, Kumar P, Warghat AR (2020) Metabolite and expression profiling of steroidal alkaloids in wild tissues compared to bulb derived in vitro cultures of *Fritillaria roylei*: high value critically endangered Himalayan medicinal herb. Ind Crop prod 145:111945. <https://doi.org/10.1016/j.indcrop.2019.111945>
- Lan X, Chang K, Zeng L, Liu X, Qiu F, Zheng W, Quan H, Liao Z, Chen M, Huang W, Liu W, Wang Q (2013) Engineering salidroside biosynthetic pathway in hairy root cultures of *Rhodiola crenulata* based on metabolic characterization of tyrosine decarboxylase. PLoS ONE 8:e75459
- Ma LQ, Gao DY, Wang YN, Wang HH, Zhang JX, Pang XB, Hu TS, Lu SY, Li GF, Ye HC, Li YF, Wang H (2008) Effects of

- overexpression of endogenous phenylalanine ammonia-lyase (PALrs1) on accumulation of salidroside in *Rhodiola sachalinensis*. *Plant Biol* 10:323–333
- Mirmazloun I, Pedryc A, Gyorgy Z, Komaromi B, Ladanyi M (2015) Glycoside content in *Rhodiola rosea* L.: dynamics and expression pattern of genes involved in the synthesis of rosavins. *Acta Hort* 1098:81–89
- Mirmazloun I, Kiss A, Ladanyi M, Gyorgy Z (2019) Production of cinnamyl alcohol glycosides by biotransformation in roseroot callus cells. *Plant Cell Tissue Organ Cult* 139:29–37
- Naik PM, Manohar SH, Praveen N, Murty HN (2010) Effects of sucrose and pH levels on in vitro shoot regeneration from leaf explants of *Bacopa monnieri* and accumulation of bacoside A in regenerated shoots. *Plant Cell Tissue Organ Cult* 100:235–239
- Nogueira RC, Paiva R, Lima EC, Soares GA, Oliveira LM, Santos BR, Emrich EB, Castro AH (2008) Growth curve and biochemical analysis of callus obtained from leaf explants of murici-pequeno (*Byrsonima intermedia* A. Juss.). *Rev Bras de Plantas Med* 10(1):44–48
- Nybakken L, Sandvik SM, Klanderud K (2011) Experimental warming had little effect on carbon based secondary compounds, carbon and nitrogen in selected alpine plants and lichens. *Environ Exp Bot* 72:368–376
- Partap M, Gupta RC, Pradhan SK (2019) Comparative analysis of morphology and phytochemical constituents in different populations and morphotypes of *Datura innoxia* Mill. and *Datura metel* L. from Punjab plains. *Asian J Pharm Clin Res* 12:193–199
- Partap M, Kumar P, Ashrita KP, Kumar D, Warghat AR (2020) Growth kinetics, metabolites production and expression profiling of picrosides biosynthetic pathway genes in friable callus culture of *Picrorhiza kurroa* royle ex benth. *Appl Biochem Biotechnol* 192(4):1298–1317
- Prasad A, Patel P, Pandey S, Niranjana A, Misra P (2020) Growth and alkaloid production along with expression profiles of biosynthetic pathway genes in two contrasting morphotypes of prickly and prickless *Solanum viarum* Dunal. *Protoplasma* 257:561–572
- Rattan S, Sood A, Kumar P, Kumar A, Kumar D, Warghat AR (2020) Phenylethanoids, phenylpropanoids, and phenolic acids quantification vis-à-vis gene expression profiling in leaf and root derived callus lines of *Rhodiola imbricata* (Edgew.). *Ind Crop Prod* 154:1–12. <https://doi.org/10.1016/j.indcrop.2020.112708>
- Schmittgen TD, Livak KJ (2008) Analyzing real-time PCR data by the comparative  $C_T$  method. *Nat Protoc* 3:1101–1108
- Shi L, Wang C, Zhou X, Zhang Y, Liu Y, Ma C (2013) Production of salidroside and tyrosol in cell suspension cultures of *Rhodiola crenulata*. *Plant Cell Tissue Organ Cult* 114:295–303
- Stepanova A, Malunova M, Salamaikina S, Selimov R, Soloveva A (2021) Establishment of *Rhodiola quadrifida* hairy roots and callus culture to produce bioactive compounds. *Phyton* 90(2):543–552
- Tao H, Wu Xu, Cao J, Peng Y, Wang A, Pei J, Xiao J, Wang S, Wang Y (2018) *Rhodiola* species: a comprehensive review of traditional use, phytochemistry, pharmacology, toxicity, and clinical study. *Med Res Rev* 39:1–72
- Tayade AB, Dhar P, Kumar J, Sharma M, Chauhan RS, Chaurasia OP, Srivastava RB (2013) Chemometric profile of root extracts of *Rhodiola imbricata* Edgew. with hyphenated gas chromatography mass spectrometric technique. *PLoS ONE* 8:e52797
- Tayade AB, Dhar P, Kumar J, Sharma M, Chaurasia OP, Srivastava RB (2017) Trans-Himalayan *Rhodiola imbricata* Edgew. root: a novel source of dietary amino acids, fatty acids and minerals. *J Food Sci Technol* 54:359–367
- Torrens-Spence MP, Pluskal T, Li FS, Carballo V, Weng JK (2018) Complete pathway elucidation and heterologous reconstitution of *Rhodiola* salidroside biosynthesis. *Mol Plant* 11:205–217
- Wahyuni DK, Huda A, Faizah S, Purnobasuki H, Wardoyo BPE (2020) Effects of light, sucrose concentration and repetitive subculture on callus growth and medically important production in *Justicia gendarussa* Burm. f. *Biotechnol Rep* 27:e00473
- Wu S, Zu Y, Wu M (2003) High yield production of salidroside in the suspension culture of *Rhodiola sachalinensis*. *J Biotechnol* 106:33–43
- Zhang JX, Ma LQ, Yu HS, Zhang H, Wang HT, Qin YF, Shi GS, Wang YN (2011) A tyrosine decarboxylase catalyzes the initial reaction of the salidroside biosynthesis pathway in *Rhodiola sachalinensis*. *Plant Cell Rep* 30:1443–1453

**Publisher's Note** Springer Nature remains neutral with regard to jurisdictional claims in published maps and institutional affiliations.